

Fully compressible time implicit hydrodynamics simulations for stellar interiors

I. Baraffe (University of Exeter - CRAL-ENS Lyon)

Exeter: Tom Constantino, Jane Pratt, Tom Goffrey
Lyon: Rolf Walder, Doris Folini, Mihail Popov
(*London* : M. Viallet)

- Motivation and challenges of computing multi-dimensional stellar structures
- The fully compressible time implicit code MUSIC
- Application to convective boundary mixing (overshooting)

Motivation for multi-D time-implicit simulations in stellar physics

Characteristics of stellar interiors:

Many (M)HD processes play key roles on stellar structure and evolution

Convection, rotation, dynamo, mixing, turbulence, etc....

- Characterised by very different timescales

Sun $\tau_{\text{dyn}} \sim (R^3/GM)^{1/2} \sim 30 \text{ min}$

$\tau_{\text{conv}} \sim 6 \text{ days}$

$\tau_{\text{thermal}} \sim GM^2/(RL) \sim 2 \cdot 10^7 \text{ yr}$

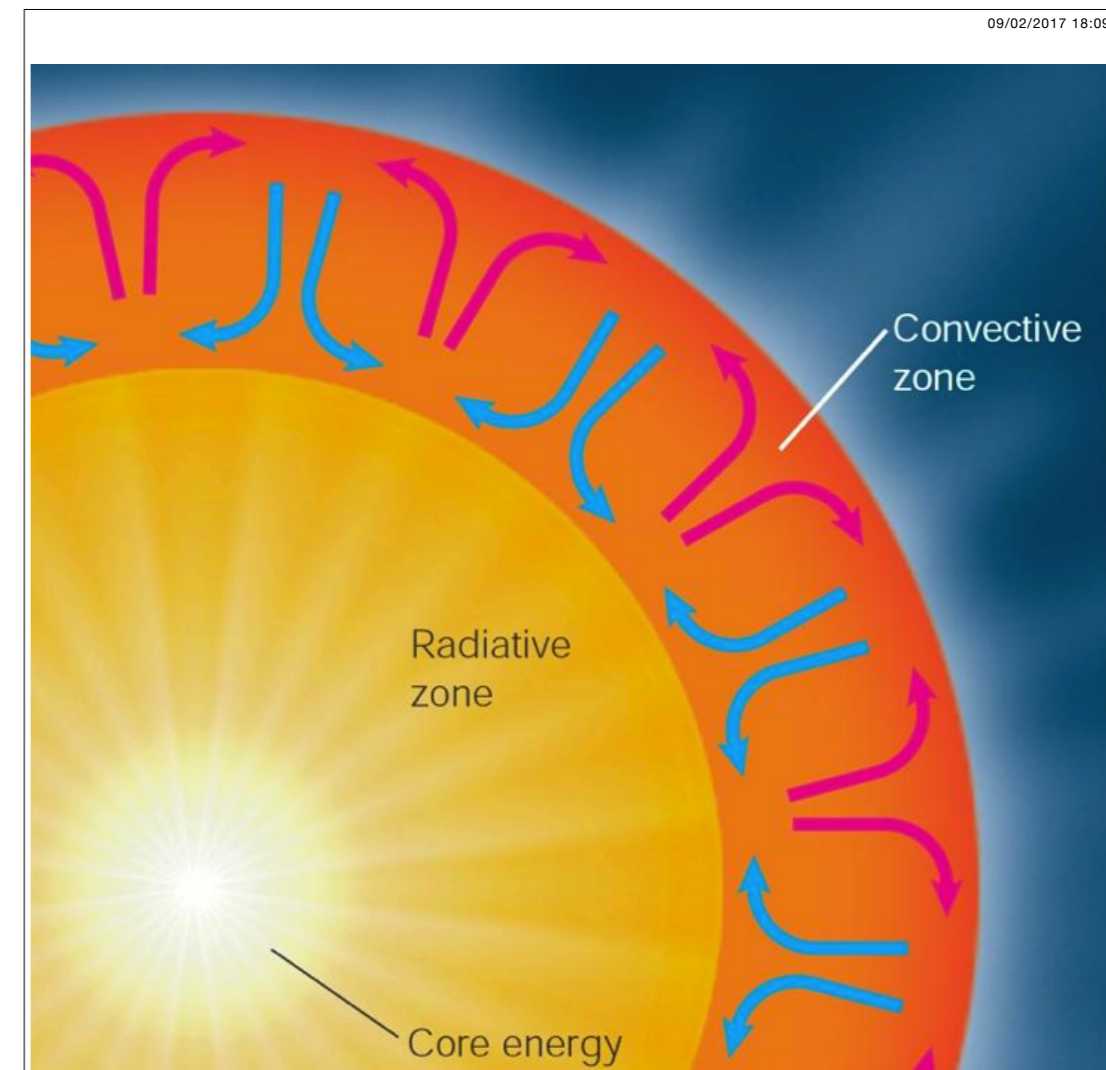
$\tau_{\text{nuc}} \sim 10^{10} \text{ yr}$

- Very different lengthscales

Pressure scale height: $H_P = dr/d \ln P$

centre: $H_P \sim R_{\text{star}}$ Surface: $H_P \sim 10^{-3} - 10^{-2} \times R_{\text{star}}$

- Range of Mach numbers ($M \sim 10^{-10} - > 1$)



😊 Many successes of 1D (spherical symmetry) models based on phenomenological approaches—→ calibration of free parameters from observations

BUT 😞 no predictive power

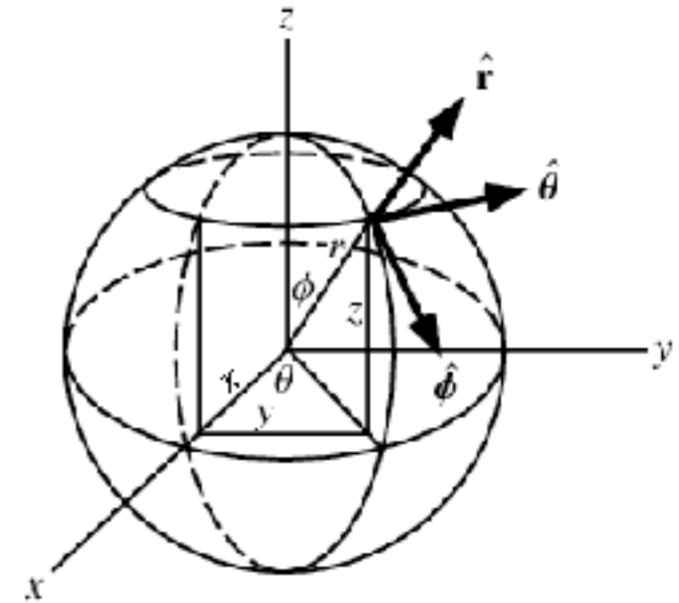
😞 degeneracy of solutions

😞 😞 do we really understand the physics?

1D Phenomenological approaches have reached their limits

⇒ **Need for multi-dimensional models**

(ideally in spherical coordinates)



Development of MUSIC “Multidimensionnal Stellar Implicit Code”

(Viallet et al. 2011, 2013, 2016; Geroux et al. 2016; Pratt et al. 2016; Goffrey et al. 2016)

- Spherical geometry (2D or 3D)
- **Fully compressible** hydrodynamics

$$\frac{\partial}{\partial t} \rho = -\nabla \cdot (\rho \vec{u})$$

$$\frac{\partial}{\partial t} \rho e = -\nabla \cdot (\rho e \vec{u}) - P \nabla \cdot \vec{u} + \nabla \cdot (\chi \nabla T)$$

$$\frac{\partial}{\partial t} \rho \vec{u} = -\nabla \cdot (\rho \vec{u} \otimes \vec{u}) - \nabla P + \rho \vec{g}$$

With the radiative conductivity $\chi = 16\sigma T^3 / 3\kappa\rho$

κ **Rossland mean opacity** (OPAL) + **realistic equation of state** (ionisation, partial degeneracy, etc...)

- Difficulty with various disparate timescales (e.g various stiff scales)

$$\tau_{\text{evol}} = \tau_{\text{therm}}, \tau_{\text{conv}}, \tau_{\text{rot}}, \tau_{\text{nuc}} \gg \tau_{\text{dyn}}$$

A standard approach is to use a time-explicit integration method:

$$\frac{du(t)}{dt} = f(u(t)) \longrightarrow u^{n+1} = u^n + \Delta t f(u^n)$$

Strictly limited by the Courant- Friedrich-Lewy condition $\Delta t < \Delta t_{\text{CFL}}$

- Hydro CFL: $\Delta t_{\text{hydro}} = \min \frac{\Delta x}{|u| + c_s}$ c_s speed of sound

- Radiative diffusion CFL: $\Delta t_{\text{rad}} = \min \frac{\Delta x^2}{k_{\text{rad}}}$ radiative diffusivity $k_{\text{rad}} = \chi / \rho c_p$

For stability: $\text{CFL}_{\text{hydro}} = \frac{\Delta t}{\Delta t_{\text{hydro}}} < 1$ **and** $\text{CFL}_{\text{rad}} = \frac{\Delta t}{\Delta t_{\text{rad}}} < 1$

• Advective timescale: $\Delta t_{\text{adv}} = \min \frac{\Delta x}{|u|}$

Stability limit for anelastic method $\text{CFL}_{\text{adv}} = \frac{\Delta t}{\Delta t_{\text{adv}}} < 1$

• **Advantage of a time-implicit method:**

$$\frac{du(t)}{dt} = f(u(t)) \longrightarrow u^{n+1} = u^n + \Delta t f(u^{n+1})$$

No stability limit on the time-step

→ adapted for problems with various stiff scales

Time step choice is driven by accuracy and physical considerations

The equations

$$\frac{\partial}{\partial t} \rho = -\nabla \cdot (\rho \vec{u}) = R_U^\rho$$

$$\frac{\partial}{\partial t} \rho e = -\nabla \cdot (\rho e \vec{u}) - P \nabla \cdot \vec{u} + \nabla \cdot (\chi \nabla T) = R_U^{\rho e}$$

$$\frac{\partial}{\partial t} \rho \vec{u} = -\nabla \cdot (\rho \vec{u} \otimes \vec{u}) - \nabla P + \rho \vec{g} = R_U^{\rho \vec{u}}$$

More compactly

$$\frac{dU}{dt} = R_U(X), \quad U = (\rho, \rho e, \rho \vec{u}) \quad X = (\rho, \epsilon, \vec{u})$$

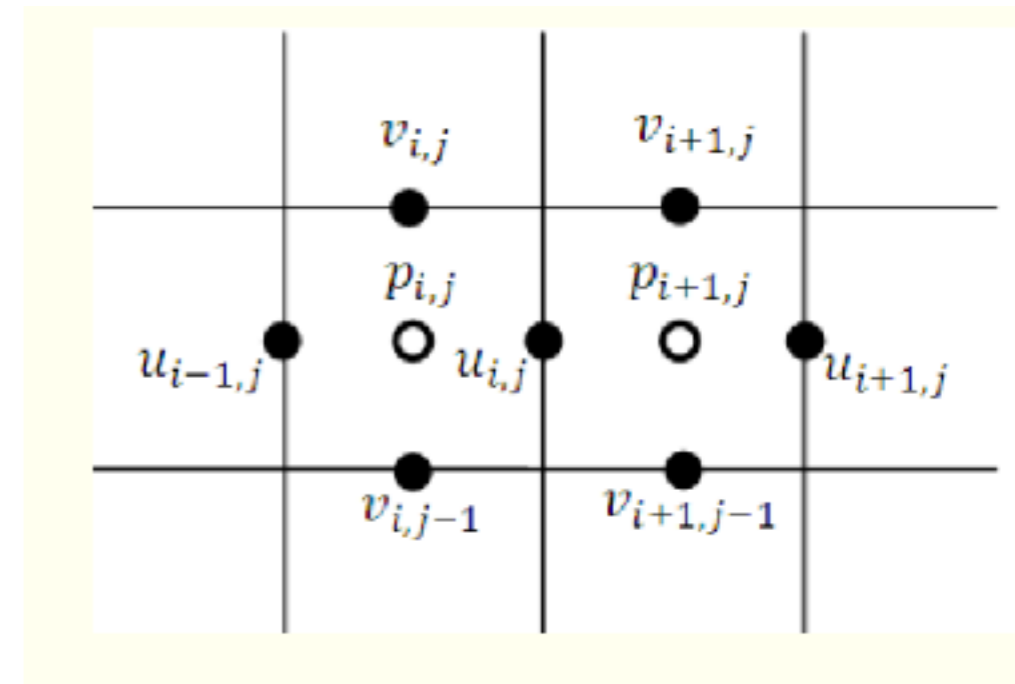
Time implicit

$$U(X^{n+1}) = U(X^n) + \frac{\Delta t}{2} (R_U(X^n) + R_U(X^{n+1}))$$

Newton-Raphson method and at each Newton iteration, solve a linear problem:

$$\underline{\mathbf{J} \delta \vec{X} = -F_U(X)}$$

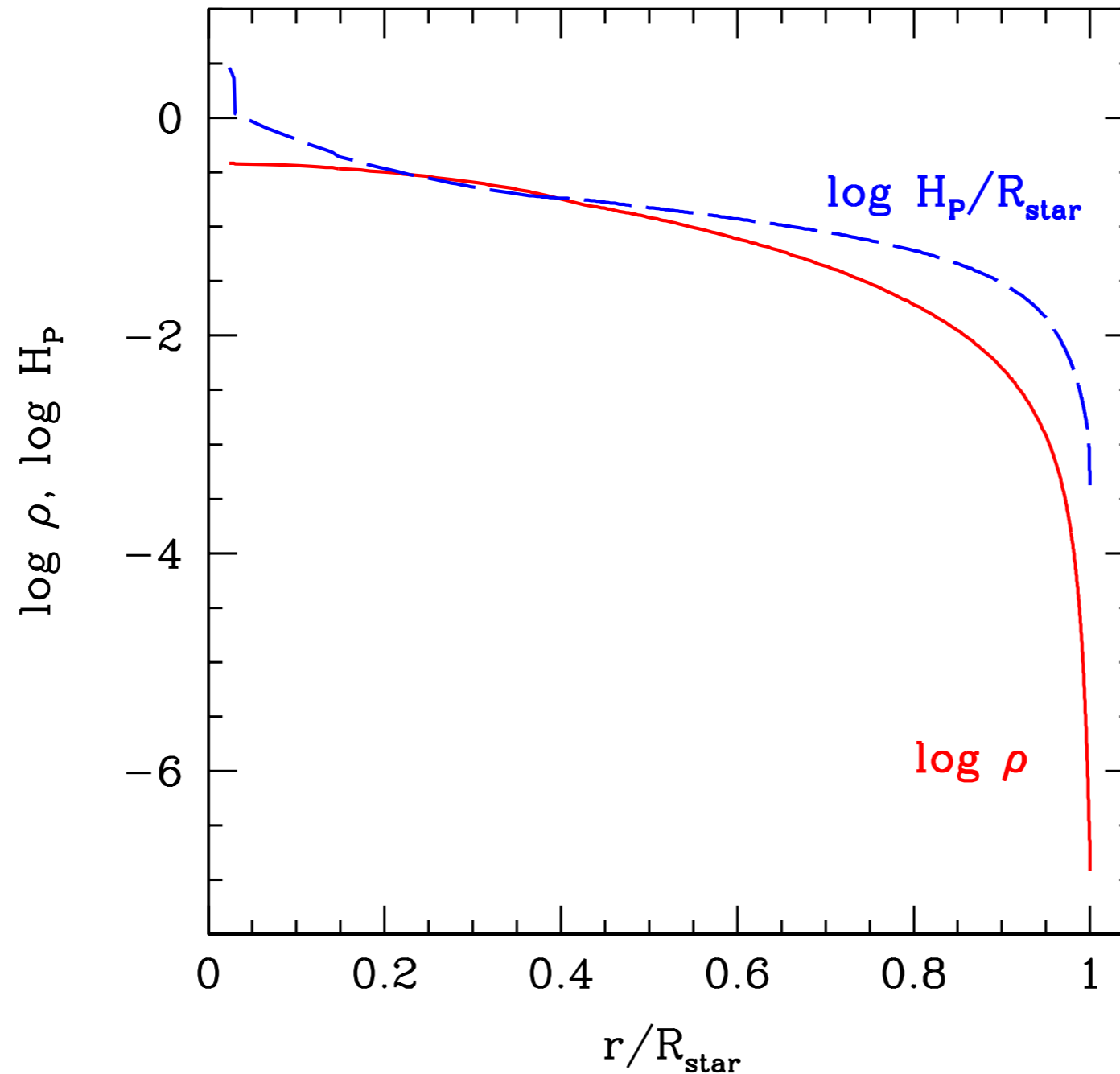
- Low storage Jacobian-Free-Newton-Krylov solver (Knoll & Keyes 2004)
(Jacobian is not stored and matrix-vector products are estimated with finite-differencing)
(Viallet et al. 2016; Goffrey et al. 2017)
- Benchmark tests (Rayleigh-Taylor, Kelvin Helmholtz, Taylor-Green vortex)
 - **Accurate for a wide Mach number range $M \sim 10^{-6} - 1$**
(Goffrey et al. 2017)
- Finite volume method on a staggered grid
(really helps for hydrostatic equilibrium $\nabla P = -\rho g$)



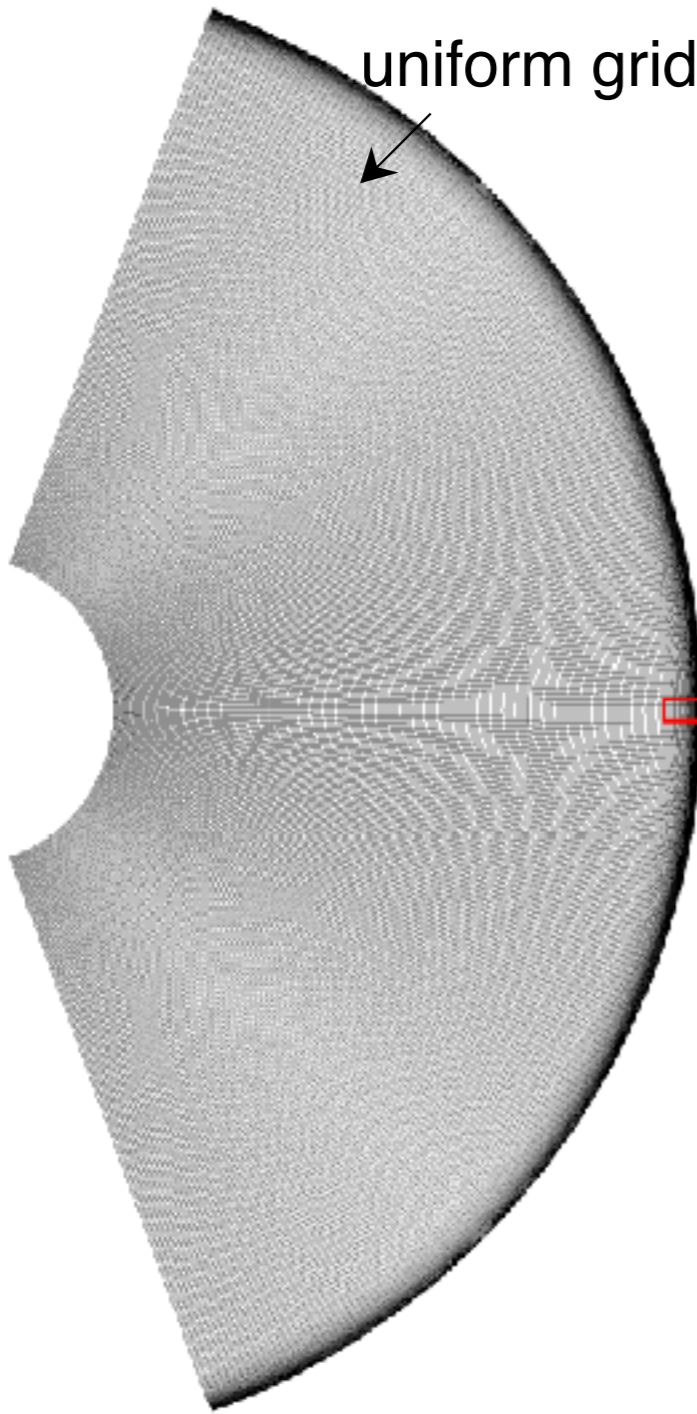
- Initial model from 1D stellar evolution calculation
 - *interface with Lyon code (Baraffe et al.) and MESA*

- **Other specificity (difficulty) characteristic of stellar interiors:**

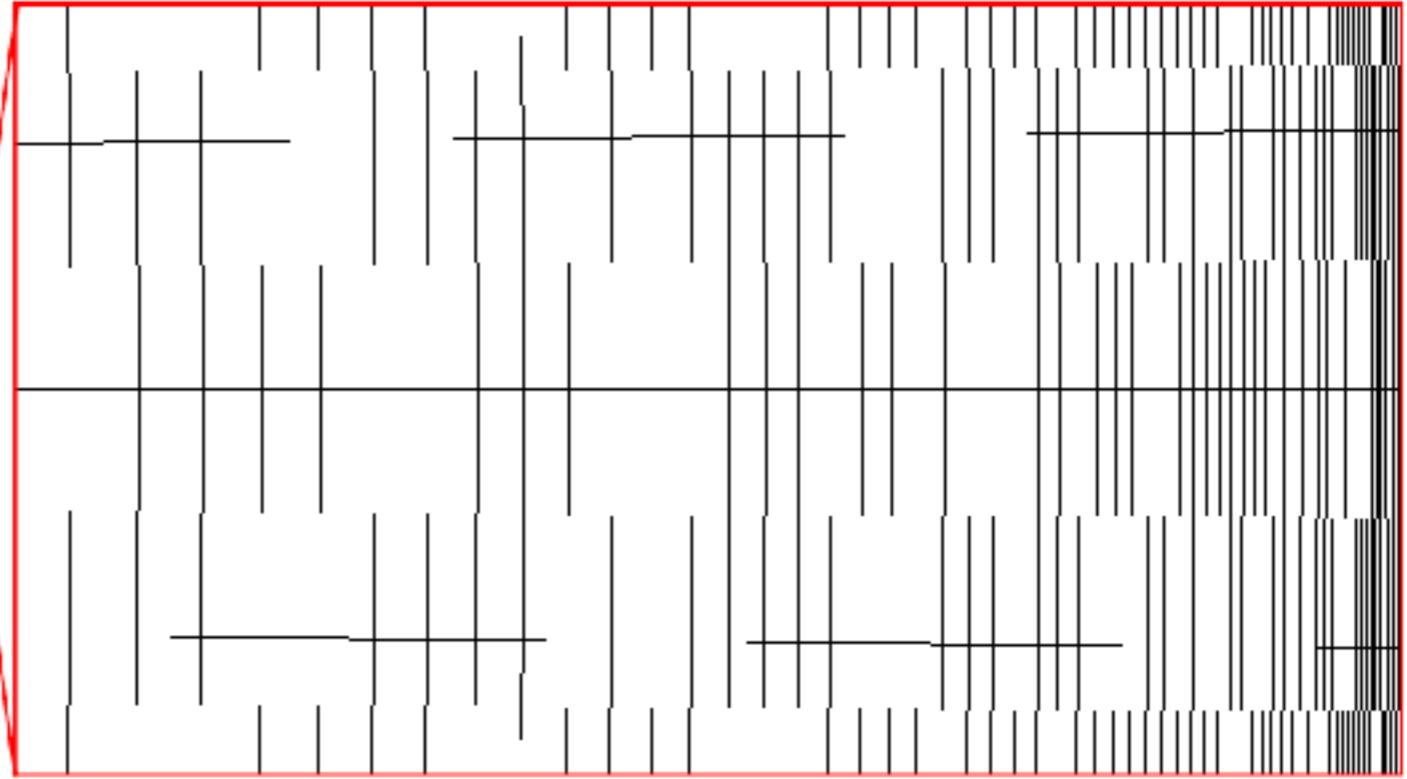
- Very different spatial scales from the centre to the surface:
pressure scale height H_P varies by several orders of magnitude
- Very steep gradients close to the surface



⇒ Use of a non-uniform grid at surface to resolve smaller scales/steep gradients



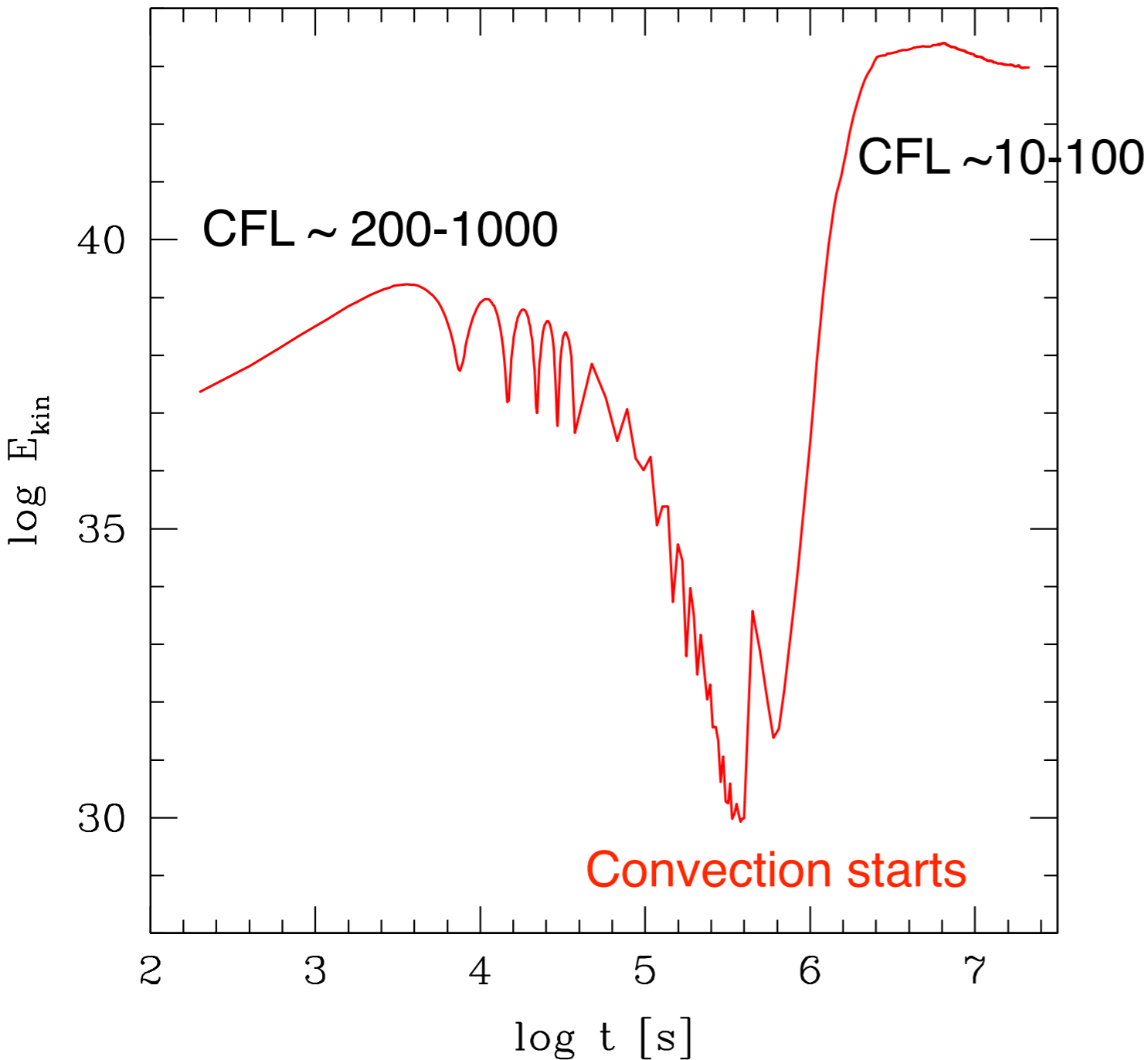
$$\Delta r_i = \Delta r_{i-1}(1 + \epsilon)$$



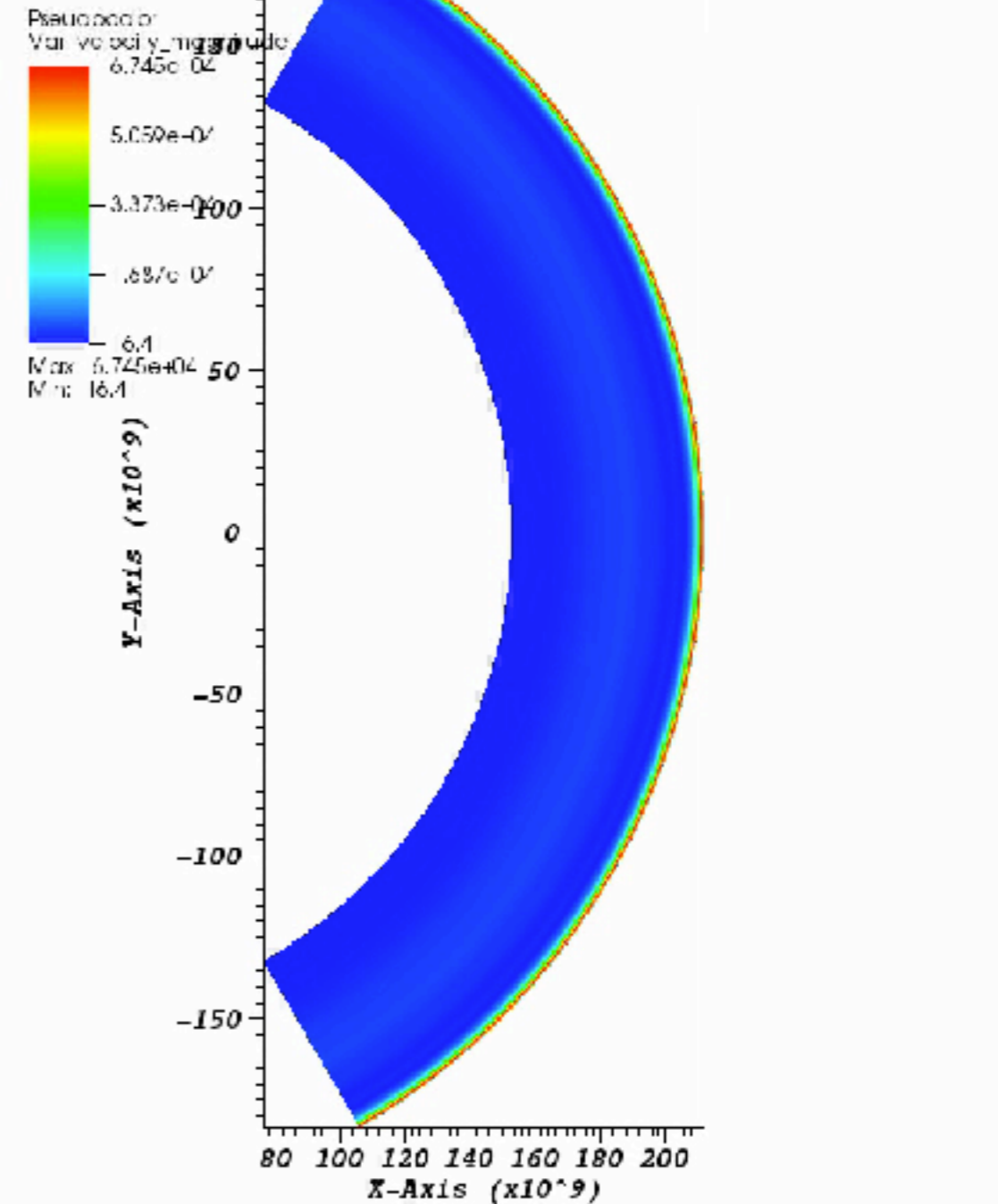
Advantage of time implicit solver → speed up the relaxation phase starting from 1D initial model (large time steps + stability)

(key to explore a range of parameters like stellar masses)

Relaxation phase from a 1D initial stellar model



DB: fort13_BC3_145x145.cont0_t000000000
Cycle: 19996



$$\text{CFL} = \Delta t / \Delta t_{\text{CFL}} \quad \Delta t_{\text{CFL}} = \min [\Delta x / (u + c_{\text{sound}})]$$

Performance of MUSIC:

Simulations of a star in 2D/3D slices from central region to surface

Example for a young (pre main-sequence) star ($1 M_{\odot}$, $\sim 60\%$ convective envelope)

- 2D simulations 256^2 ($r/R = 0.2 - 0.94$)
 ~ 10 convective turnover timescales ($\tau_{conv} \sim 10^6$ s) $\rightarrow \sim 5$ hr wallclock time with 16 procs

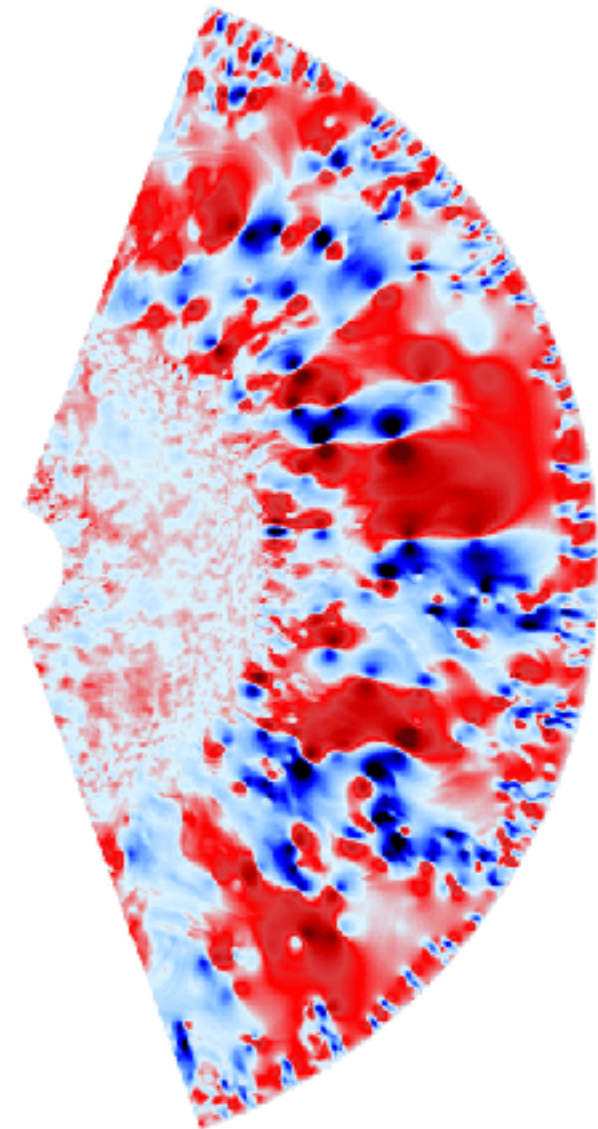
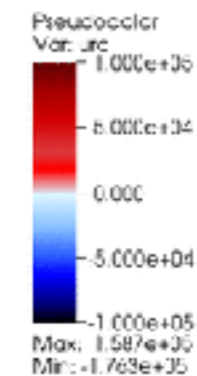
Comparison with time explicit code (A-MAZE) $\rightarrow \sim 2$ weeks wallclock time

- 2D simulations 1024^2 ($r/R = 0.1 - 1$)

256 procs, 72hr wallclock time for one τ_{conv}

- 3D simulations 256^3

with 512 procs, 6 days wallclock time for one τ_{conv}



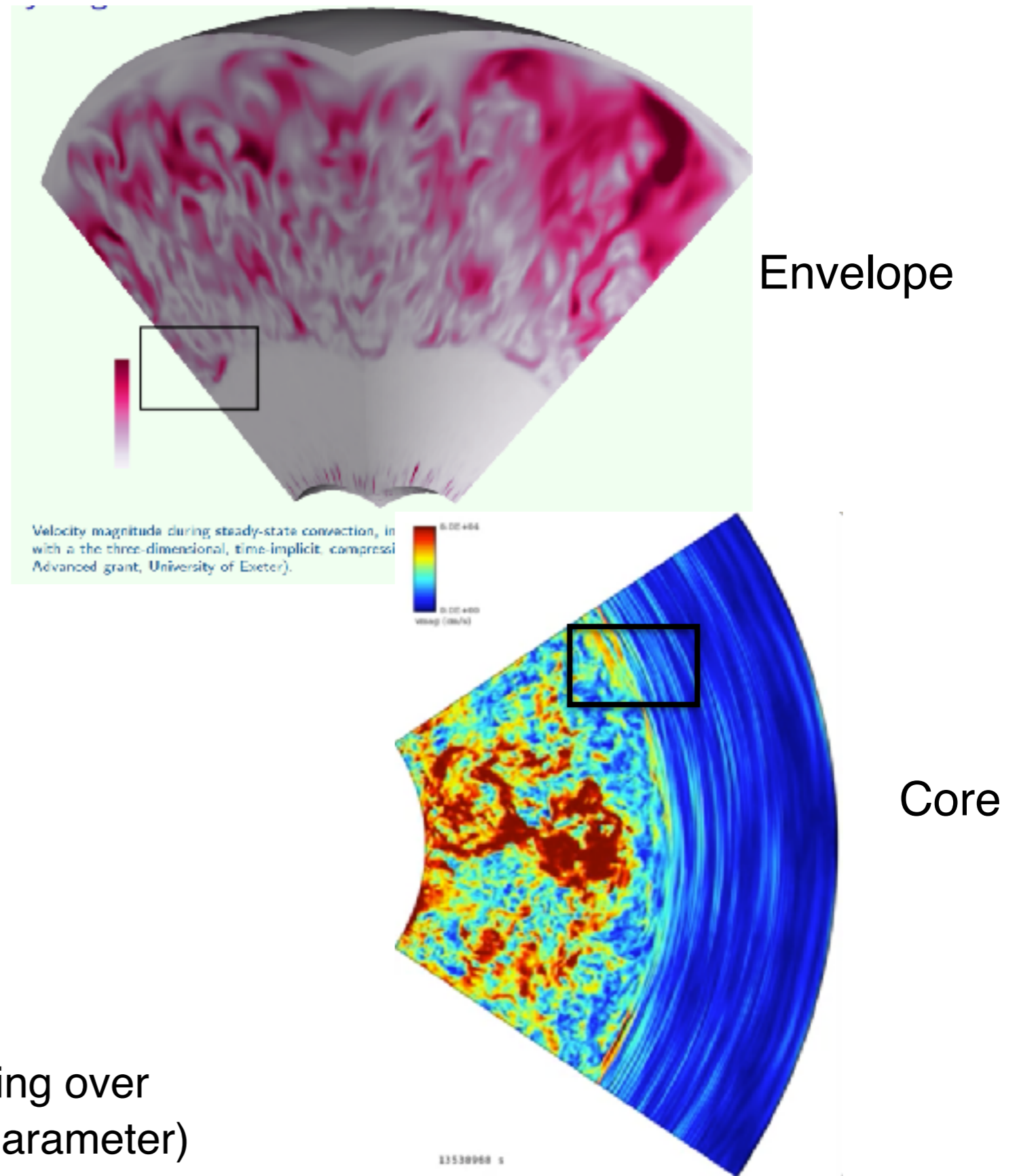
Applications to the problem of convective boundary mixing (overshooting/penetration) in stars

Long standing problem affecting chemical mixing, **age of stars**, transport of angular momentum and magnetic field.

➡ Great constraints from asteroseismology

(Roxburgh 1965; Shaviv & Salpeter 1973; Schmitt et al 1984, etc...)

Standard treatment in 1D codes: mixing over an arbitrary width $d_{ov} = \alpha H_P$ (α free parameter)

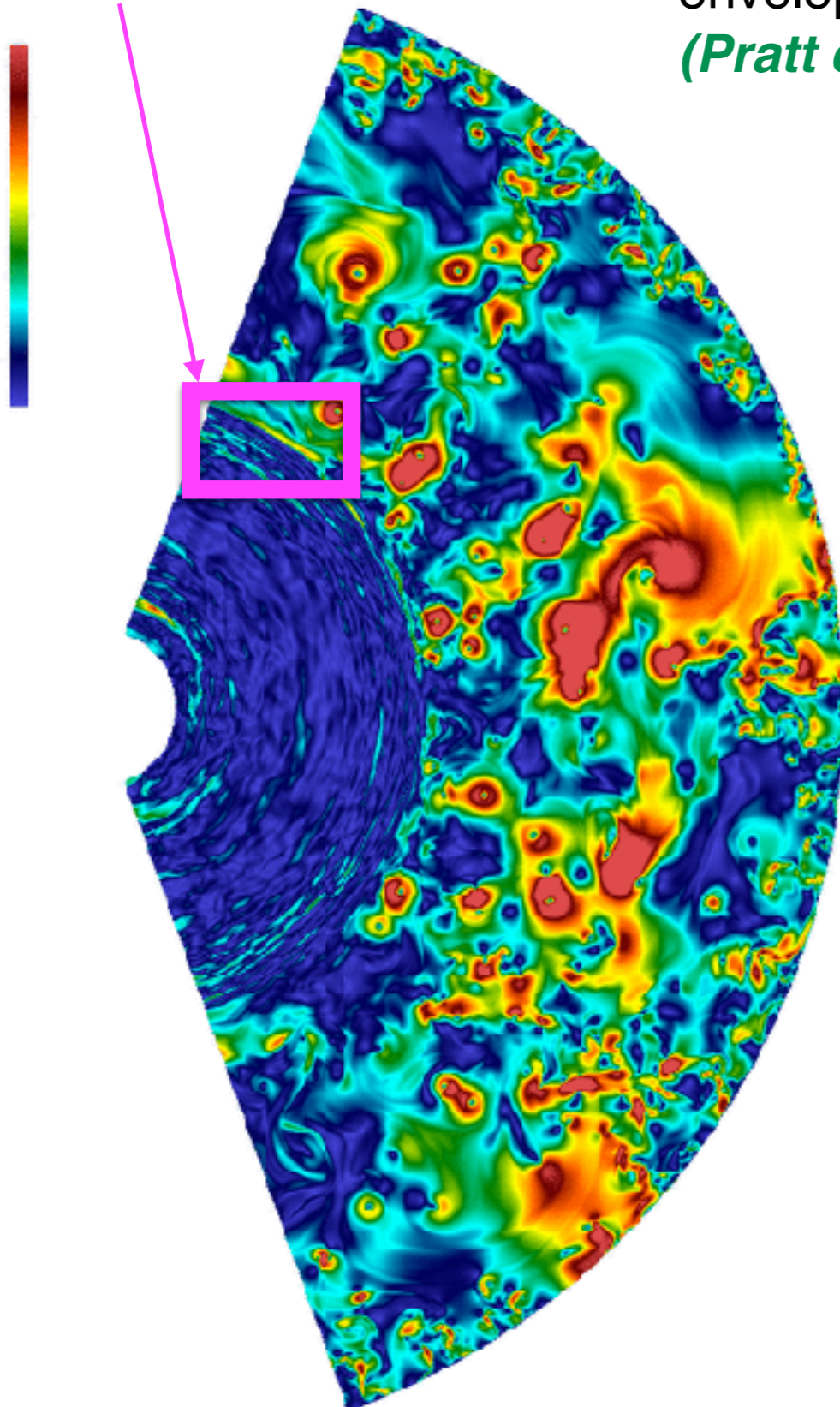


Application to convective boundary mixing in stellar envelopes

Penetration region

Convective boundary mixing

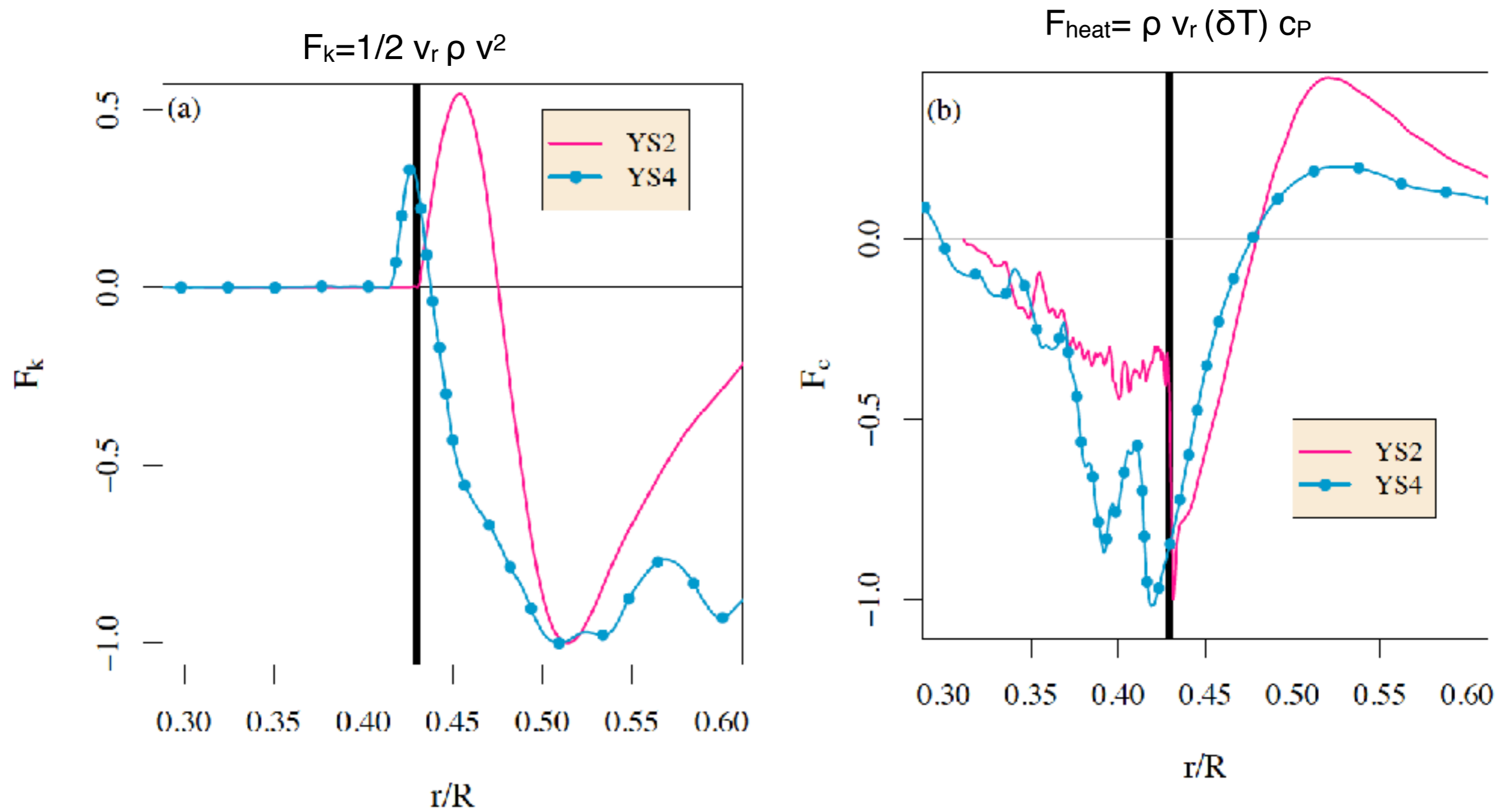
Analysis of 2D/3D simulations of a star with a large convective envelope and a radiative core (Pre-main sequence star)
(Pratt et al. 2016, 2017)



- Goal: Derivation of a **diffusion coefficient** $D(r)$ characterising the mixing in the transition region

Velocity magnitude : very high res 2432x2048

Overshooting region characterised by positive vertical kinetic energy flux and/or by change of sign of the vertical heat flux (e.g Hurlburt et al. 1994; Rogers et al. 2006)



Time-averaged and horizontally volume-averaged fluxes (usual procedure)

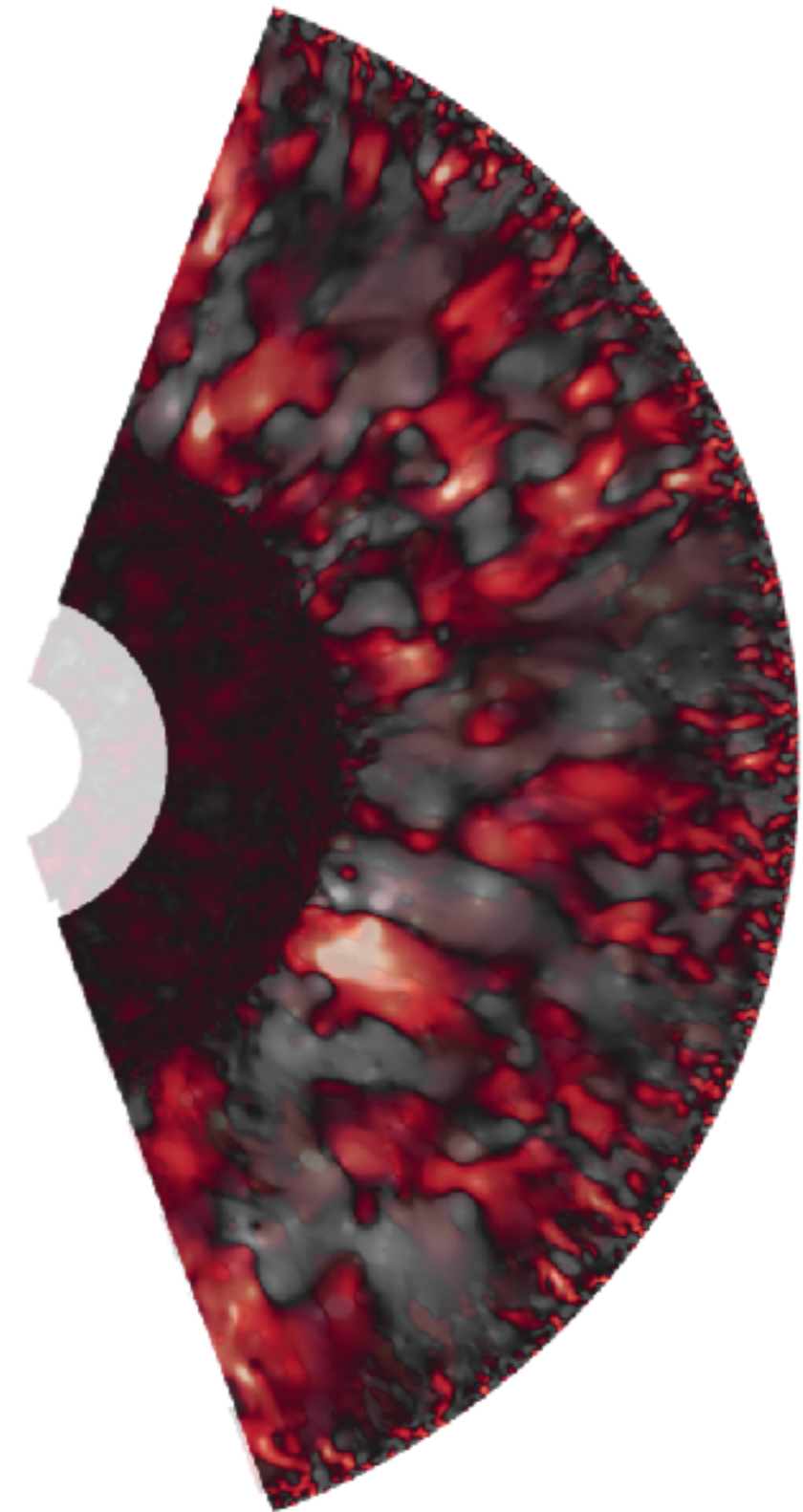
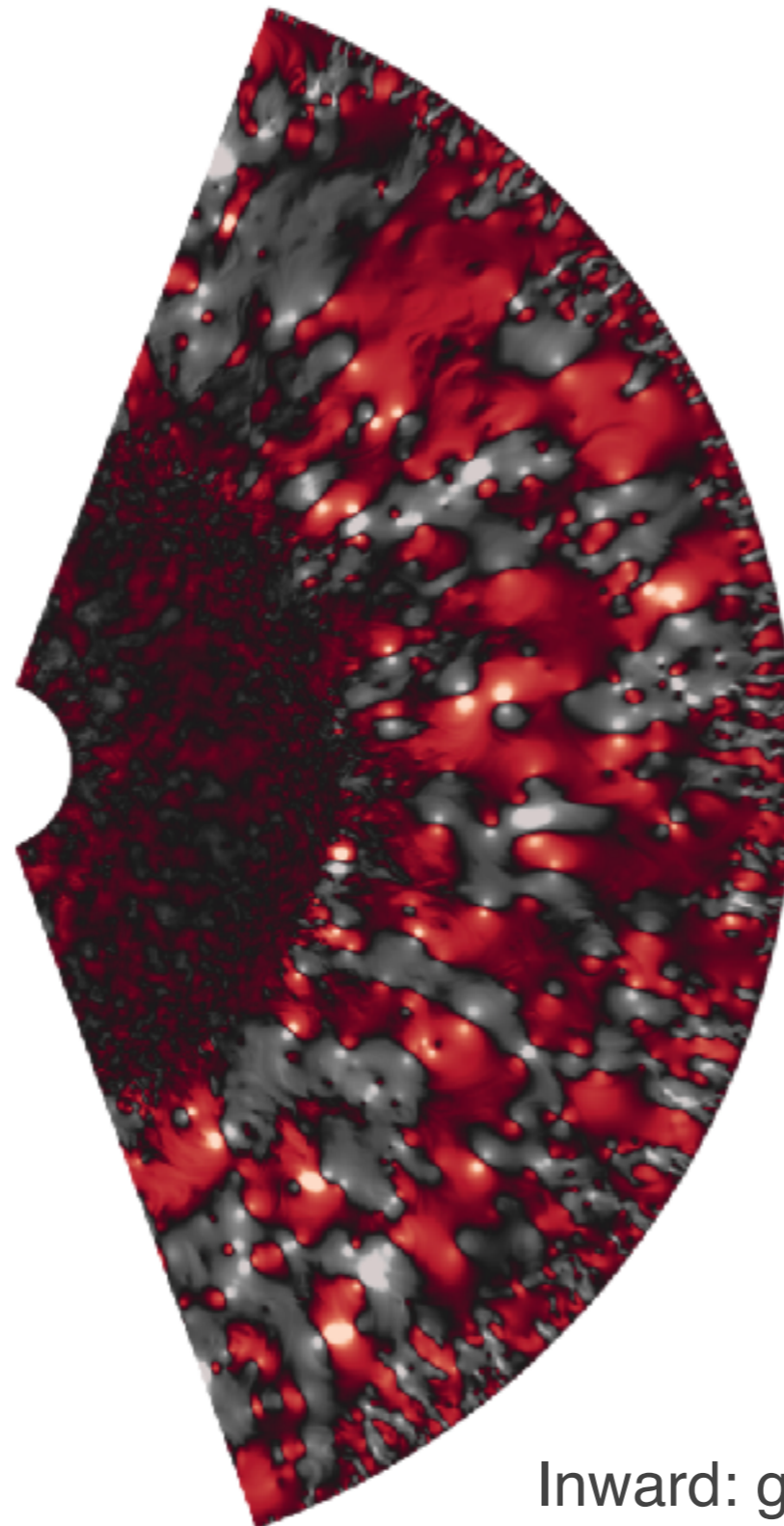
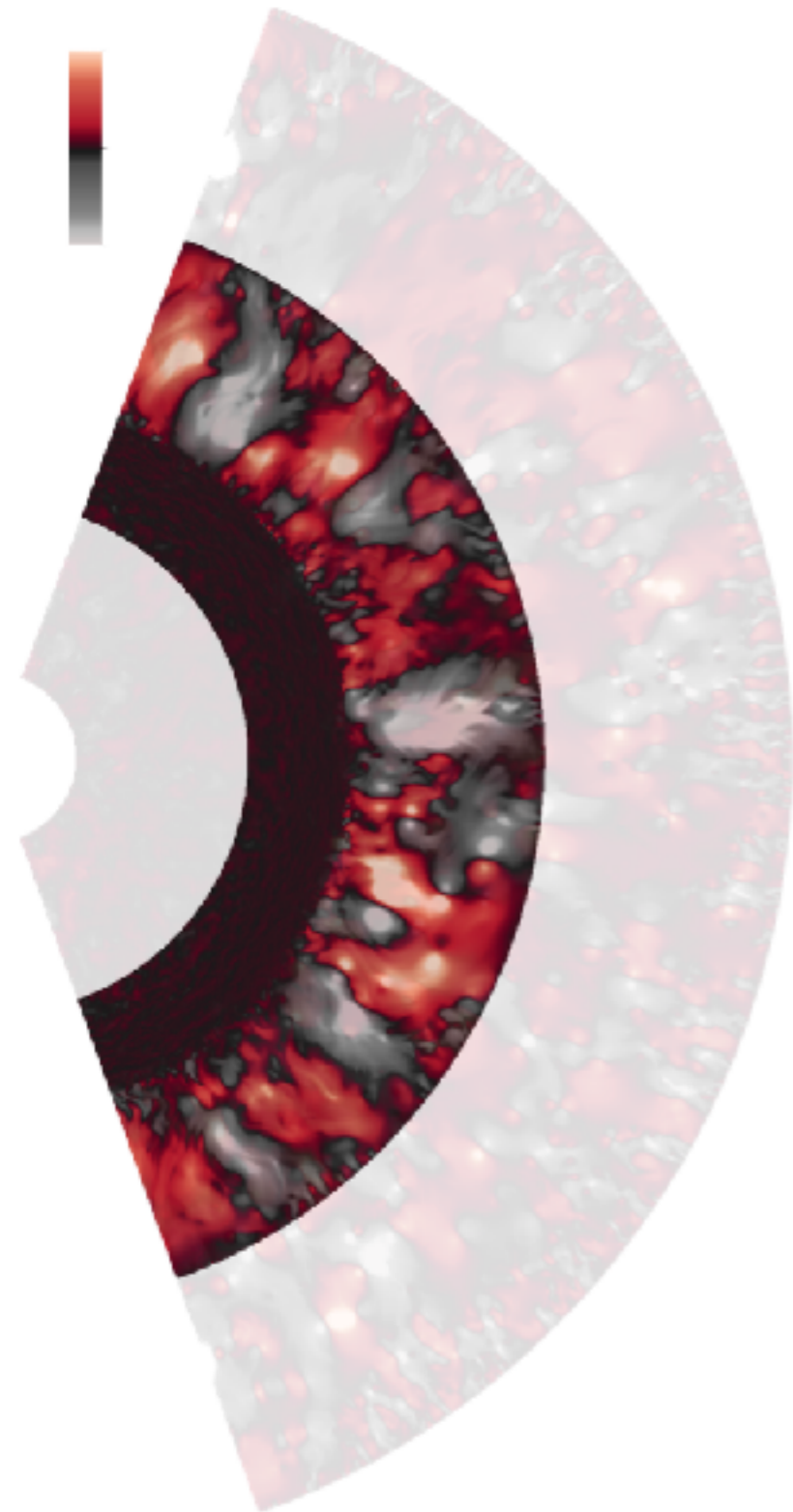
Non locality of convection: effect of the boundaries on the structures and velocities

(Pratt et al. 2016; 2017)

$r/R=0.31-0.67$

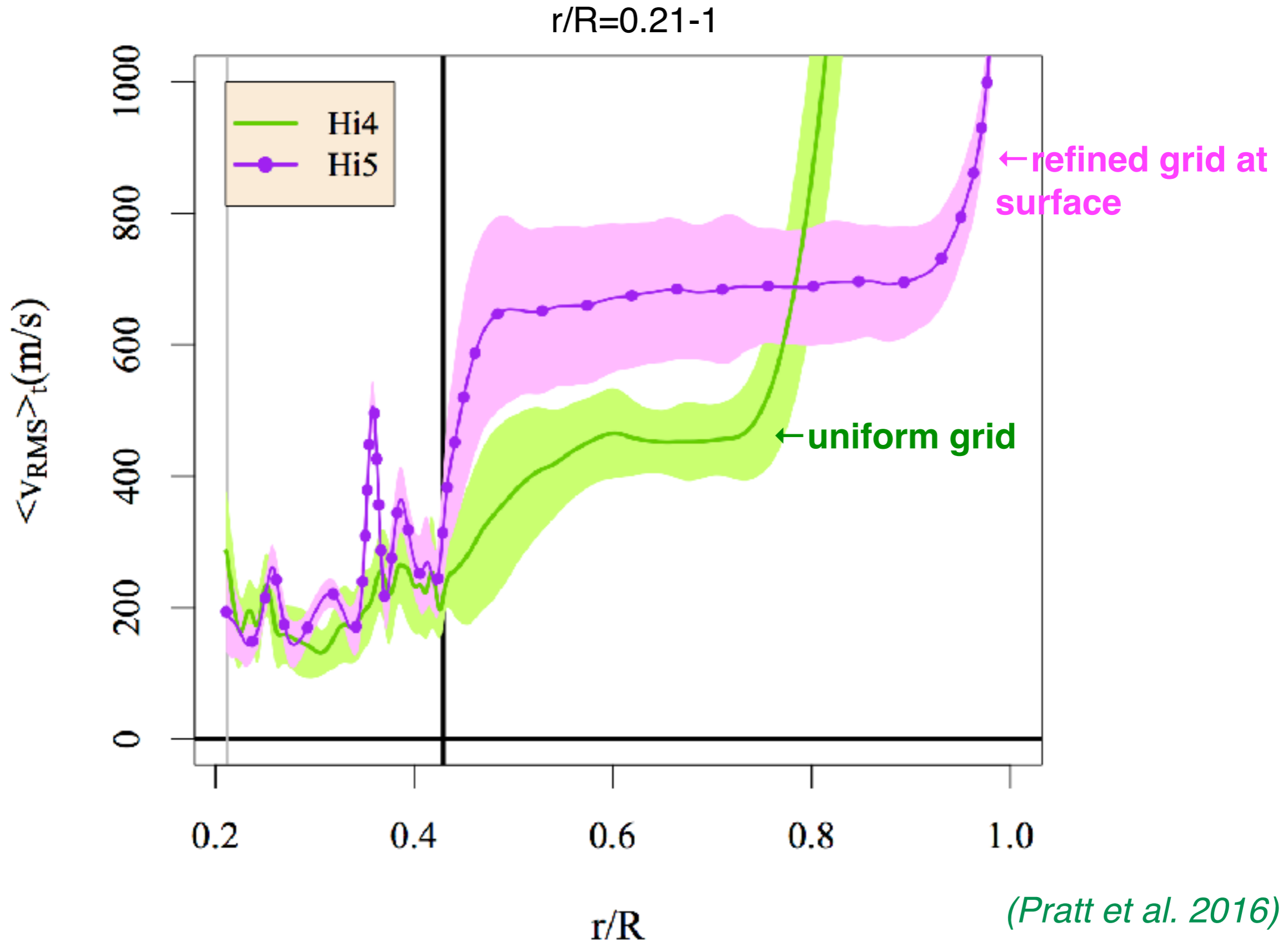
$r/R=0.1-0.97$

$r/R=0.21-1$

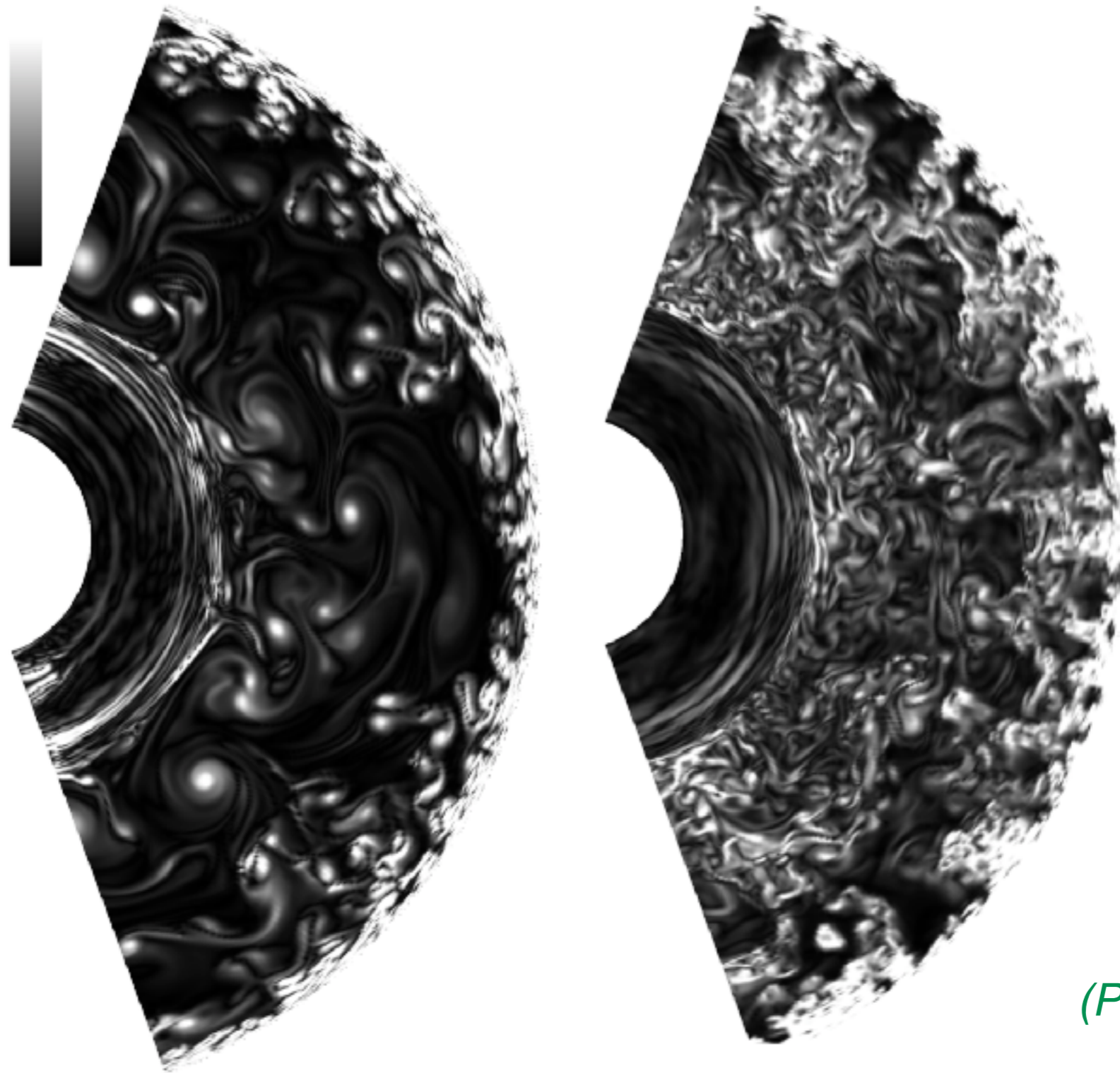


Inward: grey
Outward: red

Impact of the surface treatment on the velocities in the convective zone and at the interface convection/radiation



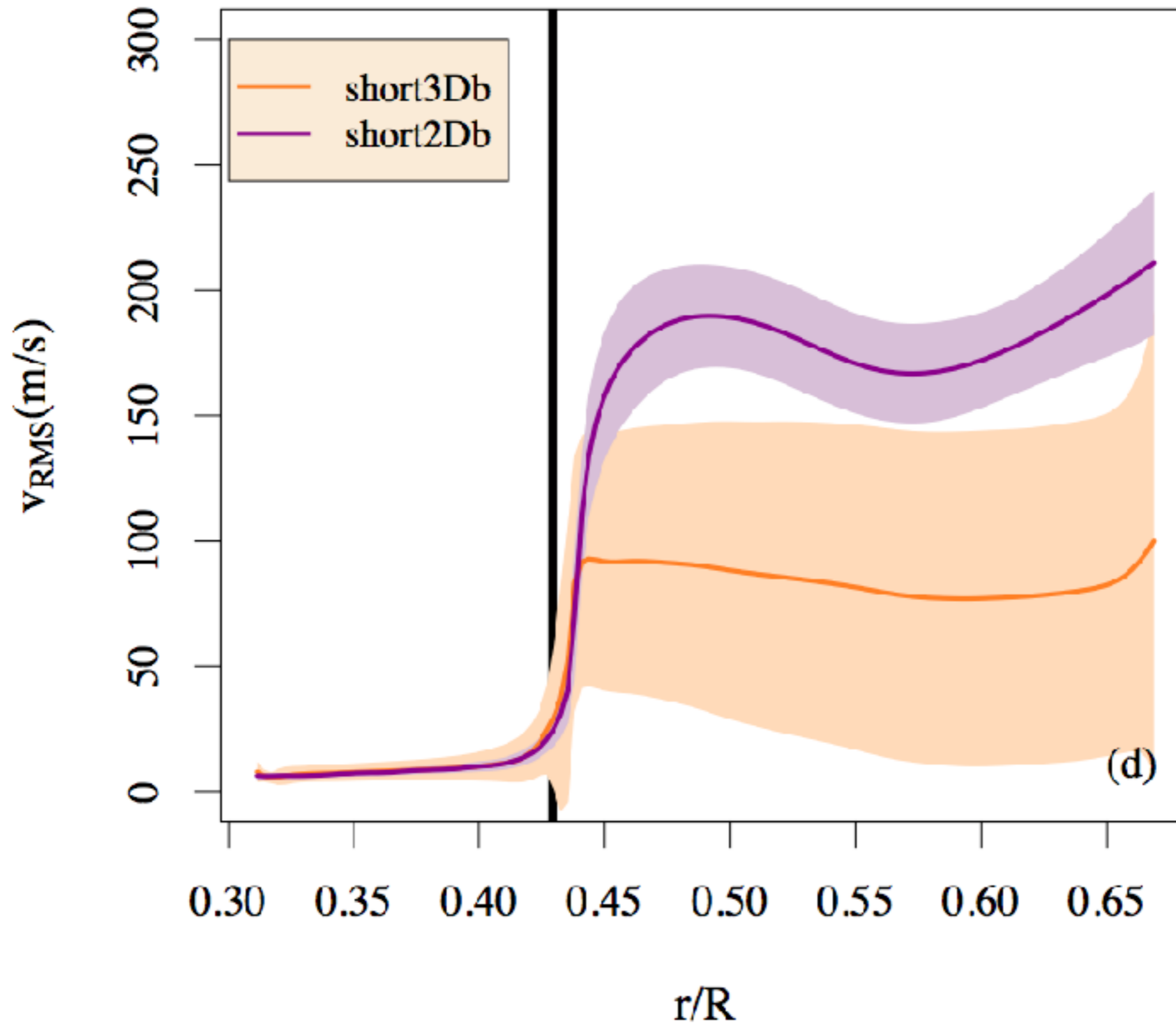
Differences between 2D and 3D simulations: vorticity magnitude



(Pratt et al. 2018)

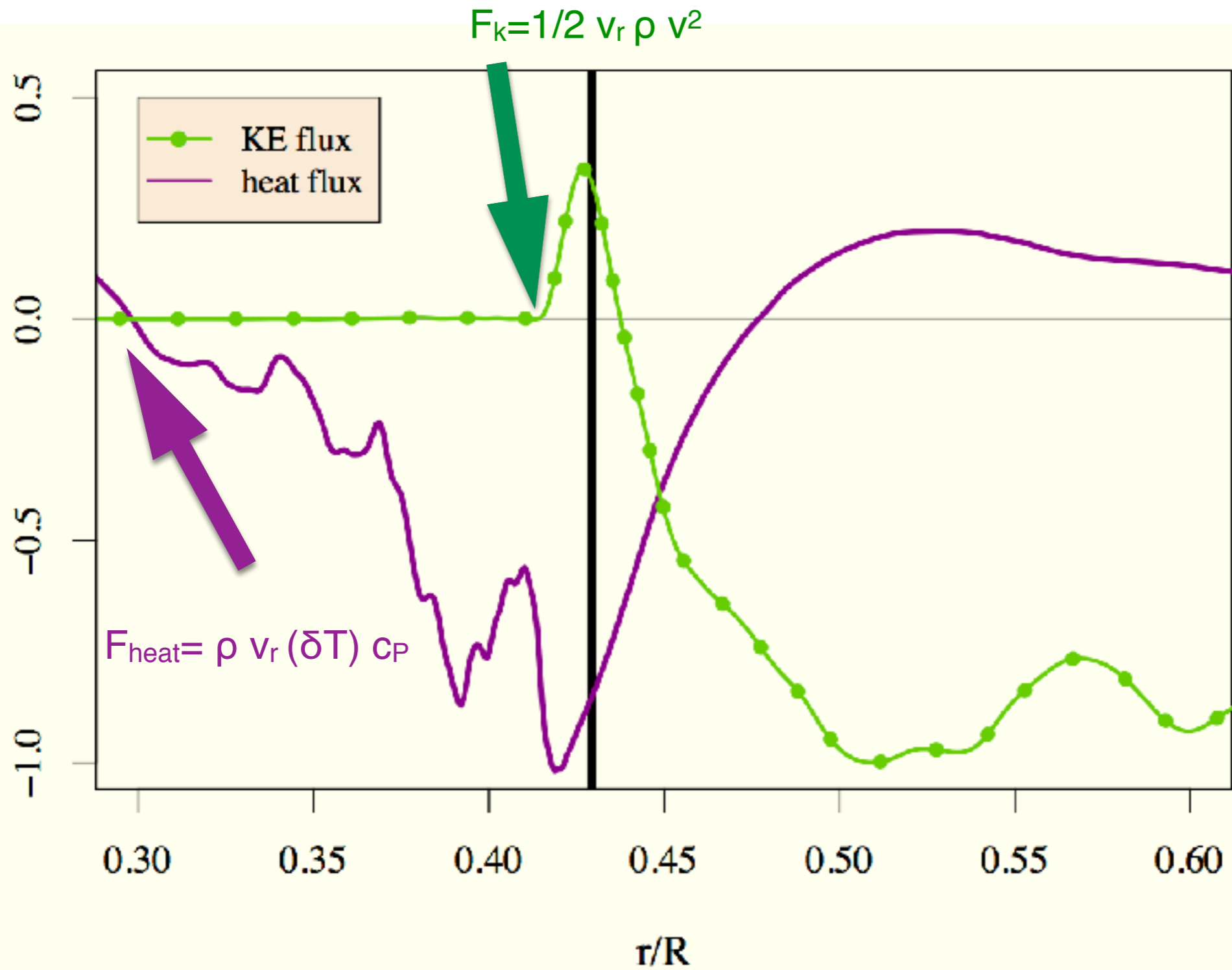
Fig. 5. Typical snapshot of the vorticity magnitude in simulation wide2D (upper left), and in a two-dimensional cut of simulation wide3D (upper right). Color scales are identical.

Differences between 2D and 3D simulations: velocity magnitude

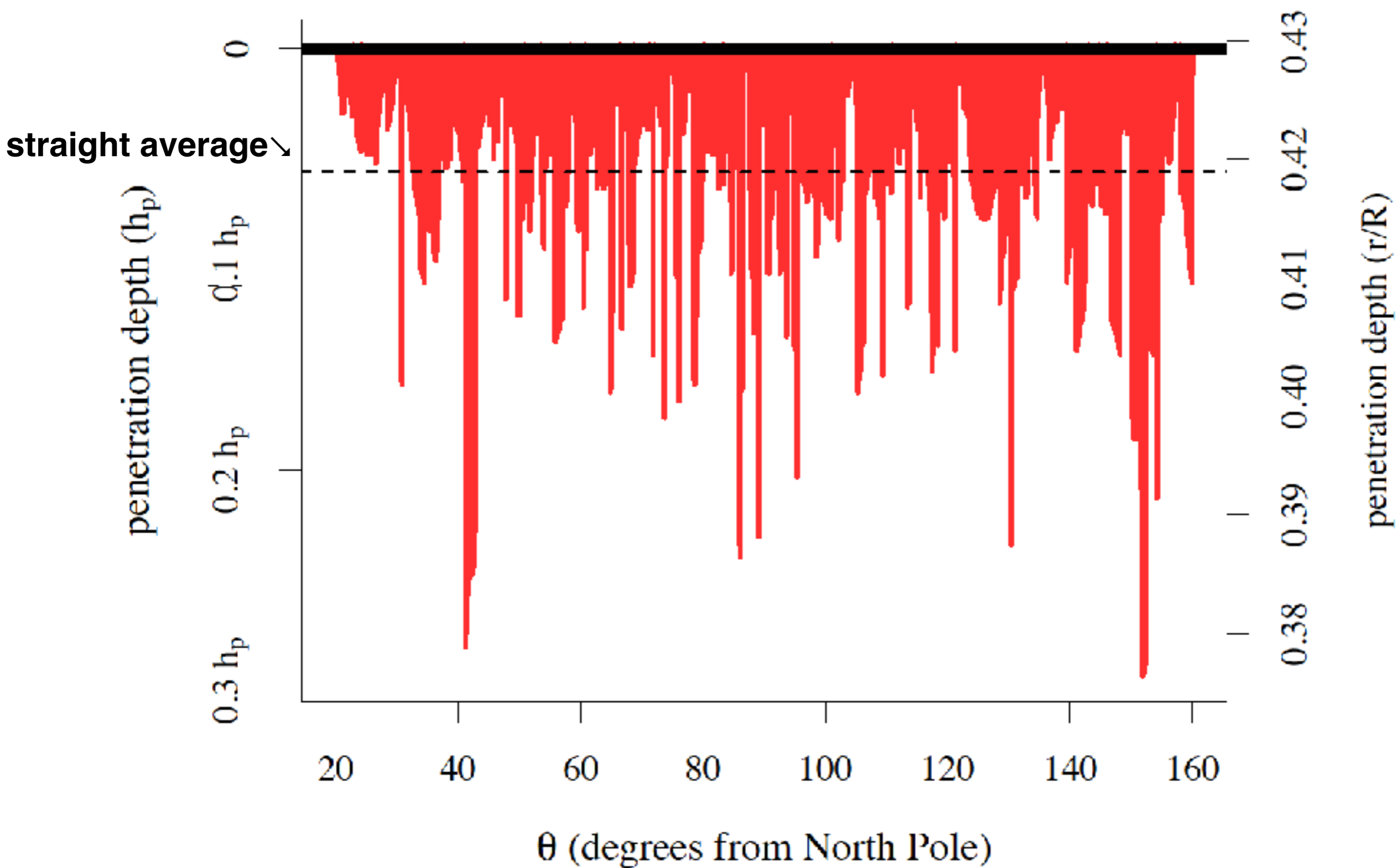


(d)

Horizontally and time-averaged F_{kin} and F_{heat} \rightarrow give different overshooting width



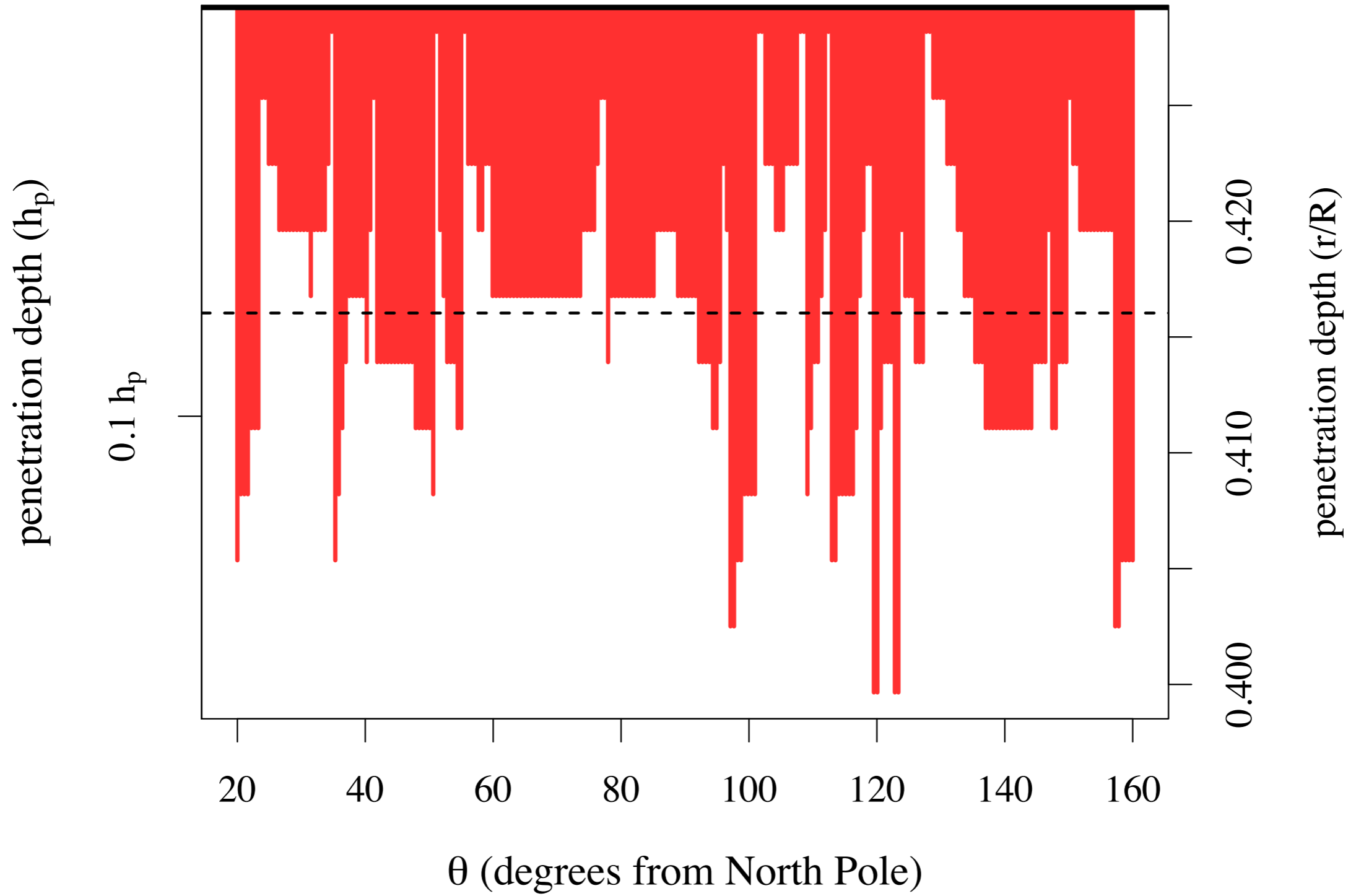
Typical shape of the penetration depths (at a given time): extent of downflows beyond the convective boundary varies with colatitude θ



➡ Straight average miss the larger penetration events

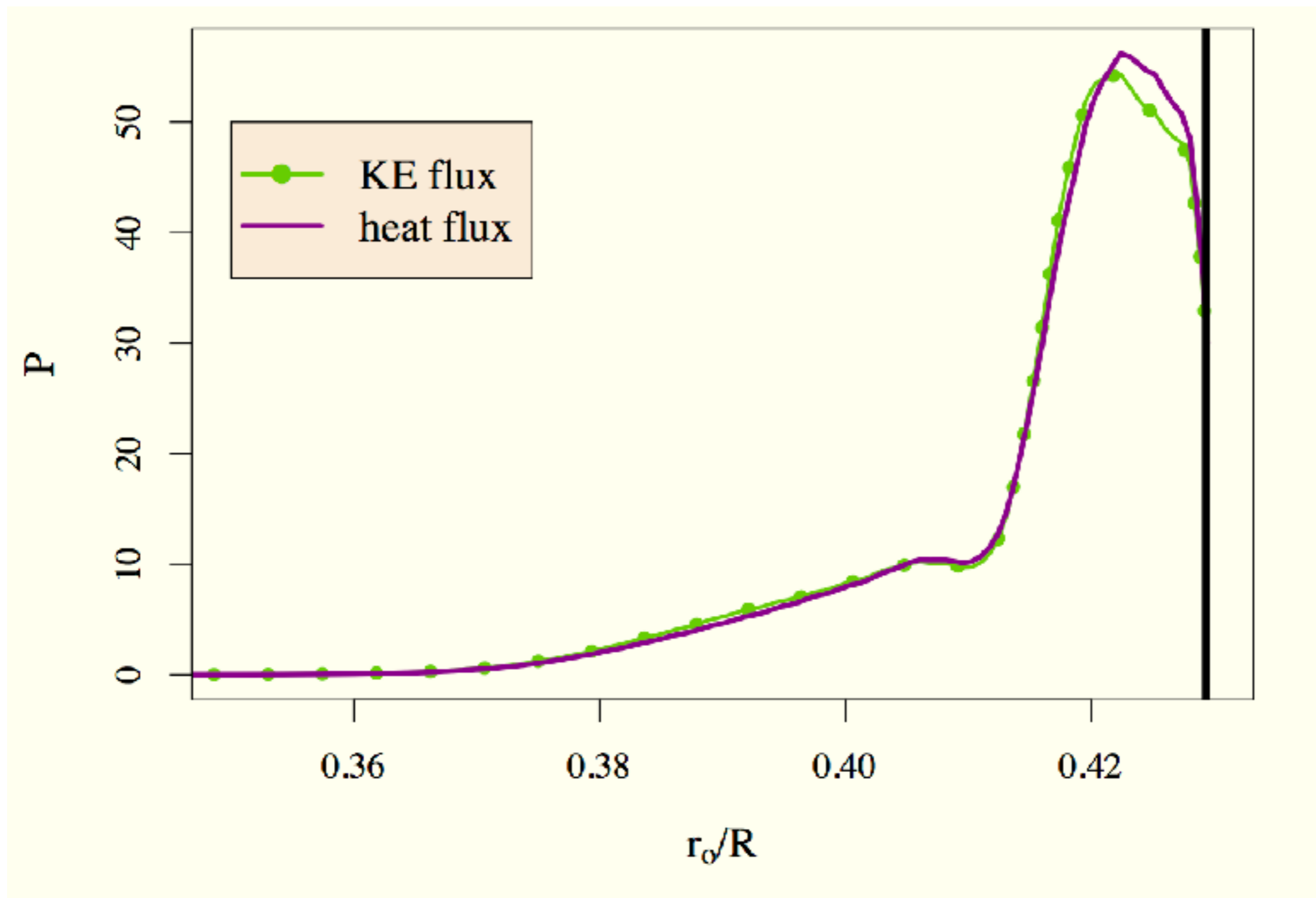
Note: Qualitatively the same picture with 3D simulations

3D 256³



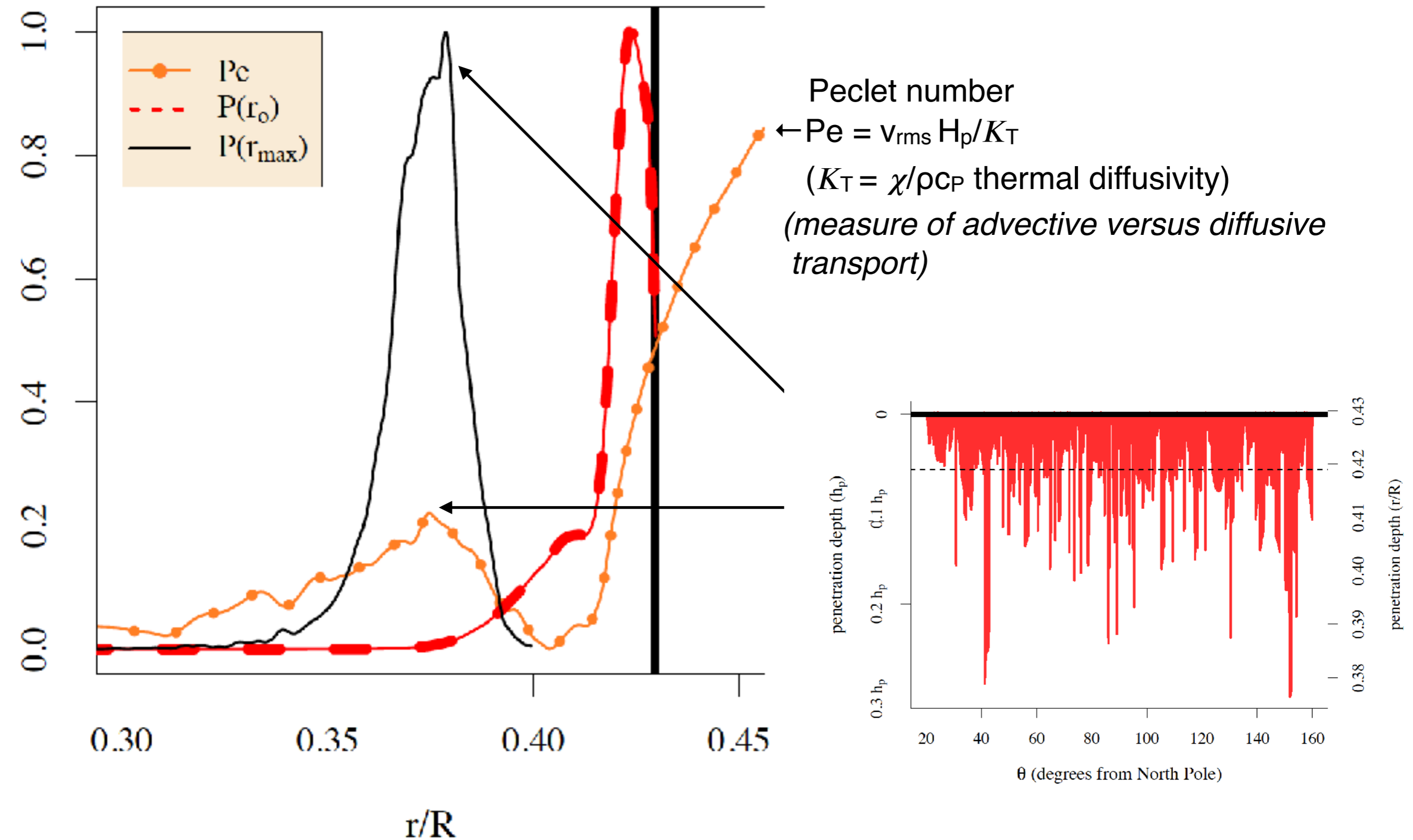
Probability Distribution of penetration depths r_0 (depth of downflows penetrating at all angles and sampled at fixed time intervals $\Delta t = 10^3 \text{ s} \sim 1/1000 \tau_{\text{conv}}$)

PDF (KE) and PDF(heat) for the same data are remarkably similar



($\tau_{\text{conv}} \sim 3 \cdot 10^6 \text{ s}$ ($\tau_{\text{dyn}} \sim 4 \text{ hr}$) - up to $500 \tau_{\text{conv}}$)

Comparison between the probability distribution (PD) of penetration depths r_0 for all downflows and the PD of maximal penetration depth r_{\max} at any time



Define a maximum penetration length $\Delta r_{\max}(t) = \max |r_0(t) - r_{\text{conv}}|$ (over all angles at a given time t)

- Distribution of maximal penetration depths, linked to extreme events in the tail of the distribution, can be described by **extreme value theory**
- Determine the probability of events that are more extreme than any previously observed (used in Earth science, traffic prediction, unusually large flooding event, finance...)

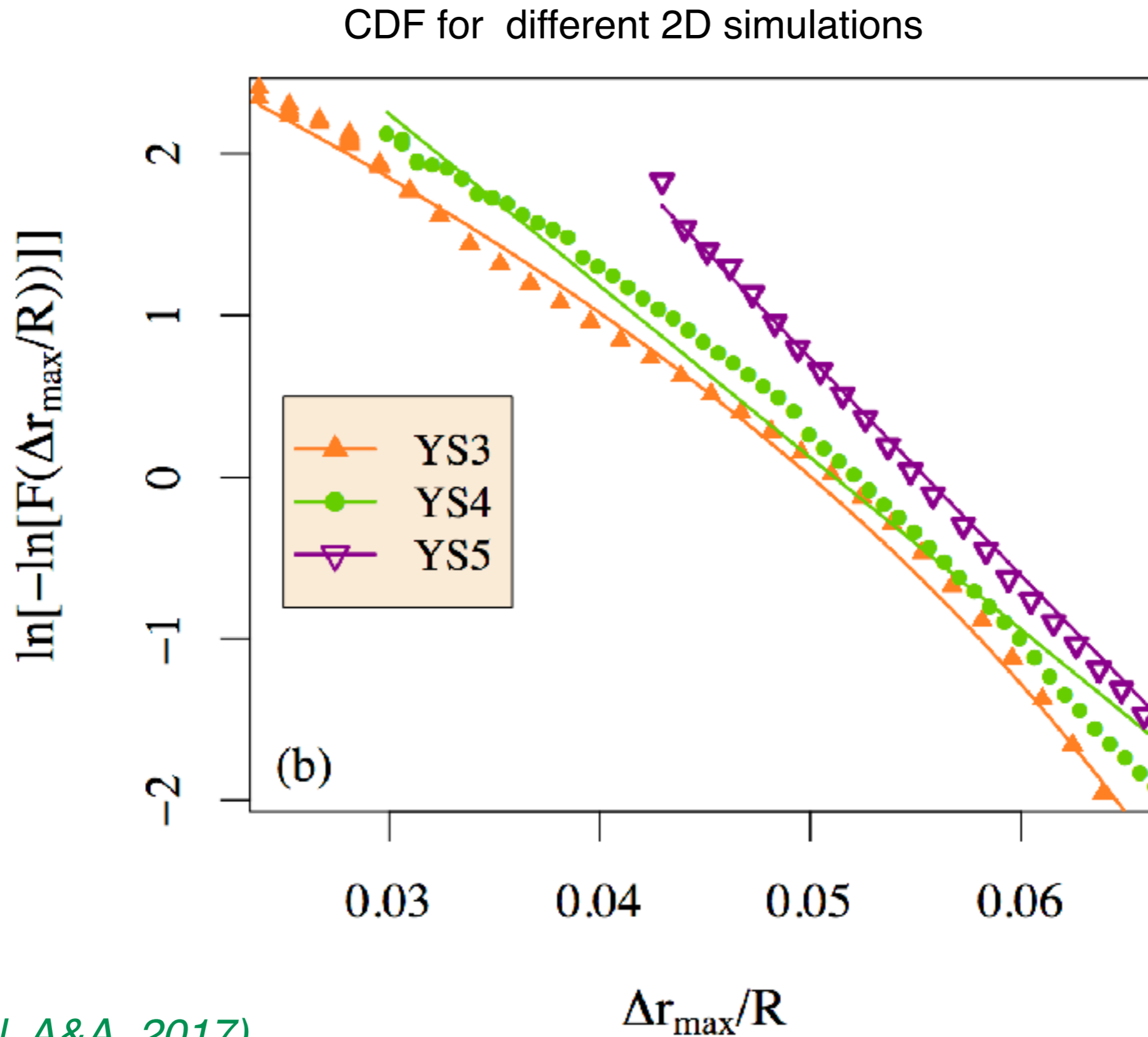
- Cumulative distribution function based on the extreme value distribution function to model the probability of maximal events has the general form:

$$F(x) = \exp\left(-\left(1 + \kappa\left(\frac{x - \mu}{\lambda}\right)\right)^{-1/\kappa}\right)$$

Where κ is defined as the shape parameter. If $\kappa=0$, the form reduces to:

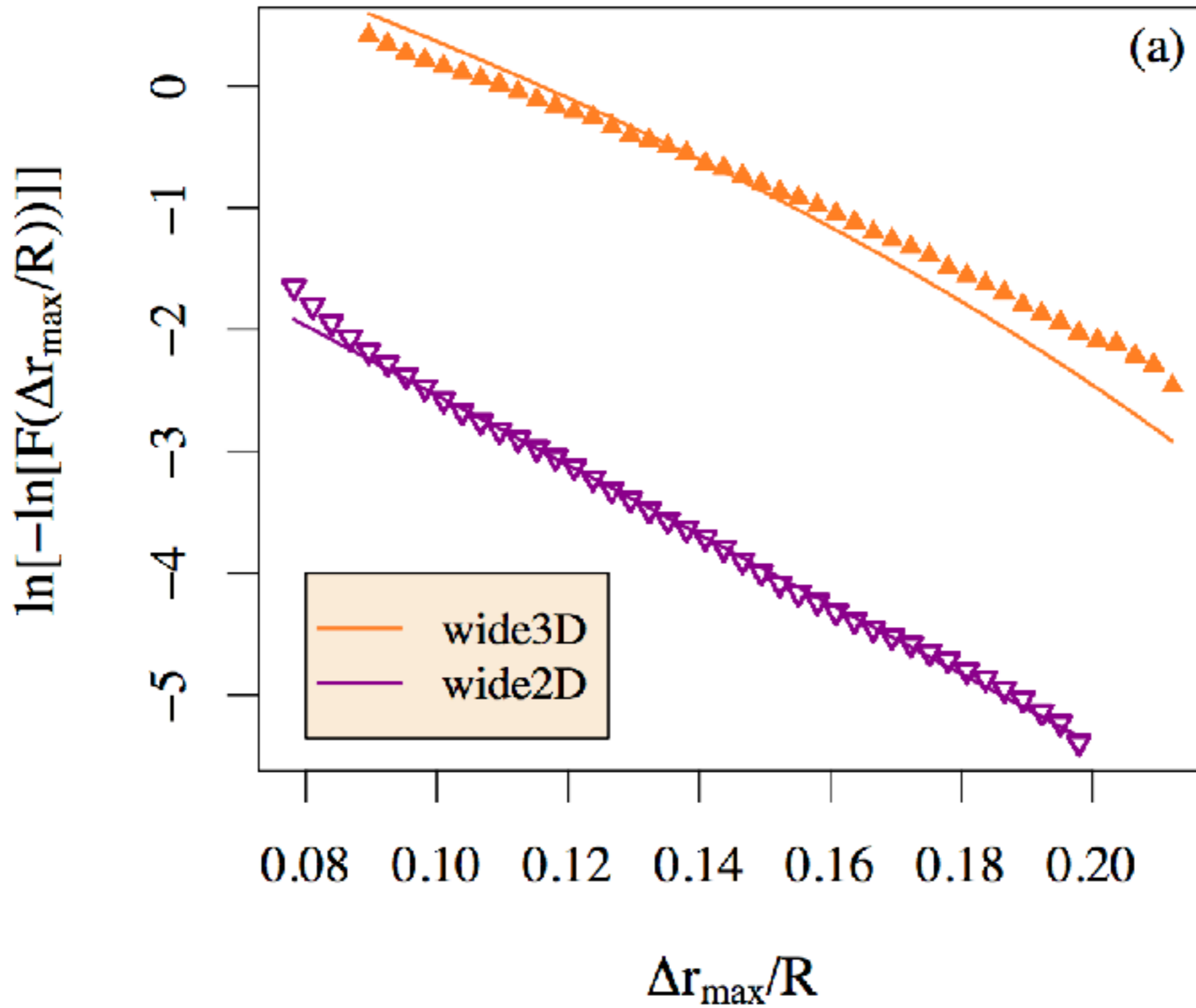
$$F(x) = \exp\left[-\exp\left(-\left(\frac{x - \mu}{\lambda}\right)\right)\right].$$

For most simulations, **best fit** given by a CDF $\propto \exp(-\exp(f(x)))$ form (with $k \rightarrow 0$).



(Pratt et al. A&A, 2017)

CDF for 2D and 3D simulations

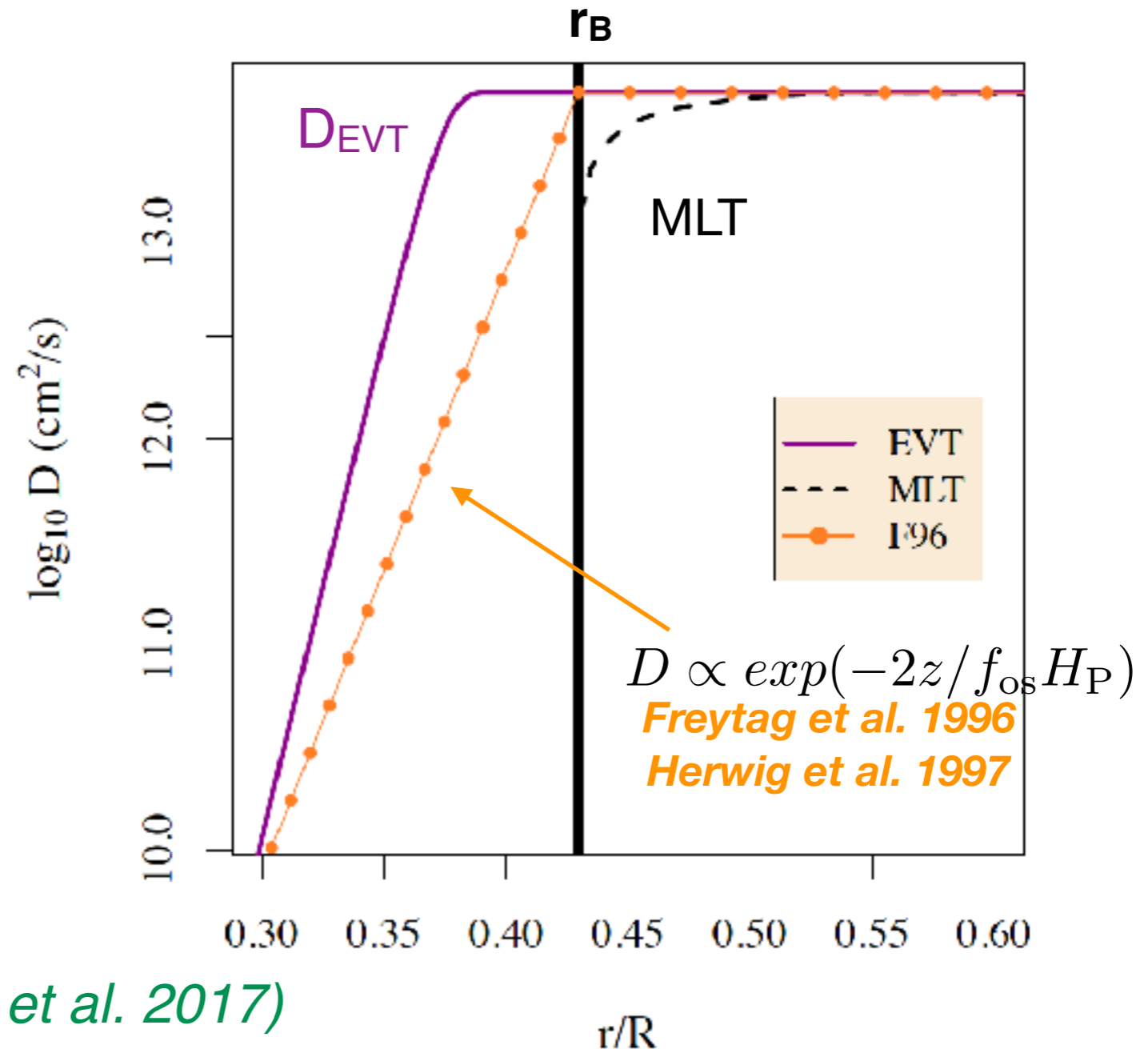


(Pratt et al. A&A, 2018)

➡ Our idea is to associate a **diffusion coefficient** to the CDF for maximum penetration events

$$D_{EVT} = D_0 \left\{ 1 - \exp \left[- \exp \left(- \frac{(r_B - r) - \mu}{\lambda} \right) \right] \right\}$$

λ, μ are predicted by simulation



(Pratt et al. A&A, 2017; Baraffe et al. 2017)

- **Envelope overshooting**
 - Extension of multi-D simulations to **different masses/ages and rotation rates**
 - Explore **MHD effects**
 - Analyse the **heat transport** in the overshooting region
- Test new convective boundary mixing formalisms against observational constraints:
 - Li as a function of age and rotation in solar type stars
 - Speed of sound profile in the transition region of the Sun
- **Extend our 2D/3D simulations to convective core overshooting:**
 - Can we apply the same statistical approach i.e presence of extreme penetrating plumes responsible for the mixing?
 - Test new transport coefficients (chemical species, heat) against asteroseismology
Search for signatures on mode properties that can be diagnosed by asteroseimology
- **Exploit the idea of statistical methods by exploring other rare even algorithms**